Carbohydrate Polymers 102 (2014) 727–737

Contents lists available at ScienceDirect

Carbohydrate Polymers

journal homepage: www.elsevier.com/locate/carbpol

Enhancement of flame retardancy and water repellency properties of cotton fabrics using silanol based nano composites

Amina L. Mohamed*, Manal A. El-Sheikh, Ahmed I. Waly

National Research Centre, Textile Division, Textile Chemistry and Technology, Department of Preparation and Finishing of Cellulosic Fibers, Tahrir Street, Dokki, Cairo, P.O. Box 12311, Giza, Egypt

ARTICLE INFO

Article history:
Received 31 August 2013
Received in revised form 24 October 2013
Accepted 30 October 2013
Available online 7 November 2013

Keywords:
Amino-functionalized silica
ZnO nano-particles
Flame retardancy
Water/oil repellency and Cotton cellulose

ABSTRACT

Environmental concerns related to fluorinated and organophosphorus compounds led to a consideration of the methods for imparting flame retardancy and water/oil repellency to textiles. A simple and facile method for fabricating the cotton fabric with superhydrophobicity and flame retardancy is described in the present work. Complex coating with amino-functionalized silica nano-particles on epoxy-functionalized cotton accompanied with ZnO nano-particles coating are carried out. In This context, new preparation techniques were used to prepare both aminated silica and ZnO nano-particles. The particle size was investigated using Transition Electron Microscope (TEM) and the chemical structure was investigated using FT-IR analysis and other analytical techniques. Cotton was functionalized with epoxy and carboxyl via grafting cotton with nano-emulsion consisted of mixture of glycidyl methacrylate (GMA) and acrylic acid (AA), and then treated for functional finishing through conventional pad-dry-cure method. The treated fabrics showed good water repellency and excellent flame retardant properties as determined by the standard test methods.

1. Introduction

Cotton is an important textile fiber used in a large range of applications. This is because cotton possesses have many characteristics that make it desirable to the consumer (Cook, 1984). One drawback of cotton is its flammability (it is easily ignited and rapidly consumed thereafter). Cotton's wide usage and the continuing implementation of flammability standards globally mean that there is a strong market need for cotton that has been made flame retardant (Powell, 1998).

Commercially, there are two main types of treatments used to impart a durable flame retardant finishing to cotton; those based on tetrakis(hydroxymethyl)-phosphonium chloride (THPC), in which the flame retardant forms an insoluble polymer that is physically trapped inside the fibers and those based on N-methylol functional phosphorous esters, in which the flame retardant is chemically bonded to the cellulose using a cross-linking resin (Powell, 1998; Stowell & Yang, 2003).

Although these and other commercial treatments are available for imparting flame retardancy to cotton, the treatments often have one or more drawbacks such as high start-up costs, licensing limitations, regulatory issues, demanding application conditions, toxic emissions and limited durability. They may also have a negative impact on the inherent, desirable properties of the fiber such as the loss of strength or resultant harsh "handle".

The challenge, therefore, is to develop innovative, eco-friendly and cost effective processes that can be employed to impart the required high performance property of, for example, flame retardancy to the cotton fiber while still preserving its natural properties.

Literature identified a number of innovative technologies available to impart high performance properties to textiles such as plasma and laser treatments, microencapsulation, supramolecular chemistry, grafting and nanotechnology (Kathiervelu, 2003; Knittel & Schollmeyer, 2000; Nelson, 2001).

One way of using nanotechnology to impart high performance properties to natural fibers, while preserving the inherent properties of the fiber, is the modification of the fiber surface by applying a nano-coating. Hybrid inorganic–organic polymers (ORMOCERs, organically modified ceramics), applied by the sol–gel coating process are well suited for this purpose (Mahltig & H.Böttcher, 2002).

Silicones have some unique properties including low surface energy, excellent lubricity, heat stability, high compressibility, low surface tension, hydrophobicity, good electric properties, low fire hazard and limited solubility in organics coupled with water insolubility (Abidi, Hequet, & Tarimala, 2007).

Another attractive character of silicon was its improvement on flammability of the polymers (Annakutty and Kishore, 1988a,

* Corresponding author. Tel.: +20 11 29 76 999 1.
E-mail addresses: alo.mohamed12@hotmail.com, alo.mohamed@yahoo.com (A.L. Mohamed).

0144-8617/$ – see front matter © 2013 Elsevier Ltd. All rights reserved.
http://dx.doi.org/10.1016/j.carbpol.2013.10.097

1988b; Banks, Ebdon, & Johnson, 1994; Liu, Hsiue, Lee, & Chiu, 1997). While heating, low surface energy of silicon renders it to migrate to the surface of the polymer and to form a protective layer with high heat – resistance to avoid polymer residue from thermal degradation. Therefore, silicon is considered as one of the environment friendly flame retarding elements, including phosphorus and nitrogen. Phosphorous compounds have been demonstrated to exhibit notable efficiency on improving flame retardancy of polymers through a condensed mechanism (Wu, Liu, & Chiu, 2002). Moreover effective synergistic effect of silicon and phosphorus on enhancing char formation and improving flame retardancy of polymers was also observed (Hsiue, Liu, & Tsiao, 2000; Hsiue, Liu, & Liao, 2001).

2. Experimental

2.1. Materials

2.1.1. Fabric

100% bleached, plain weave (poplin) (23 ends and 23 pick/Cm) was supplied by "Misr El – Beida Dyers", Egypt. The fabric was scoured with a solution containing 5 g/l sodium carbonate and 5 g/l non-ionic detergent at boil for 3 h. Then it is rinsed with hot and cold water and left to dry at ambient temperature.

2.1.2. Reagents

Glycidyl methacrylate (GMA) and diethylphosphit were obtained from Across. 3-Aminopropyltriethoxysiliane (APTES) was obtained from Fluka, acrylic acid (AA) and silicon dioxide powder were purchased from Sigma–Aldrich. Toluene and methanol were analytical grade and purchased from lobachemie (India). Ammonium ferrous sulphate and hydrogen peroxide were bought from Fluka. Zinc acetate, sodium hydroxide, chloroacetic acid, sodium carbonate, isopropanol and ethanol are analytical grade chemicals. Carboxymethyl starch (CMS) with degree of substitution (DS) of 0.2 was prepared according to a reported method (El-Sheikh, 2010).

2.2. Methods

2.2.1. Synthesis

2.2.1.1. Synthesis of amino functionalized silica nanoparticles. The attachment of amino groups onto the silicon dioxide surface was achieved by the condensation reaction between surface silanol groups and 3-aminopropyltriethoxysilane. Into a 2000 ml round flask, 30 g of silicon dioxide and 1000 ml of 10% solution of 3-aminopropyltriethoxysilane in toluene (v/v) are mixed, and the silicon dioxide particles were homogenously dispersed by a magnetic stirrer for 30 min. 100 ml of methanol:water (2:1) are added to the mixture and stirred for 72 h. The modified silicon dioxide particles were filtrated and extracted with toluene for 24 h using soxhlet extractor to remove untreated 3-aminopropyltriethoxysilane. The APTES treated silicon dioxide was dried in an oven at 60 °C for 24 h and stored in a desiccator. The nano size functionalized silicon dioxide particles were mechanically prepared, where 15 gm of dried particles were dispersed in 100 ml toluene then mixed using a high speed homogenizer (IKA, Ultra Turrax, USA) at 24,000 rpm. The solution is subjected to twice 120 s homogenizer at room temperature (23–25 °C) and is repeated ten times. The produced powder was freeze-dried for 48 h at −40 °C (Lyotrap Plus, LTE Scientific, UK) to obtain a fine powder of amino functionalized silica, which was then kept in desiccators.

Aminated silica nano-particles were characterized by transmission electron microscopy (TEM), and FT-IR spectroscopy techniques.

2.2.1.2. Synthesis of nano size ZnO. ZnO NPs were prepared using Zinc acetate as a precursor and CMS as a stabilizing agent. The process of the preparation could be described as follows:

10 g of CMS are dispersed in 200 ml distilled water in a stoppered bottle and kept under stirring till complete dissolution. 55 g of Zn acetate were dissolved in distilled water and added gradually to the CMS solution under continuous stirring using magnetic stirrer. 10 g of sodium hydroxide were dissolved in distilled water and allowed to cool to room temperature. The aqueous sodium hydroxide solution was then added gradually to the CMS/Zn acetate mixture under stirring. A milky cream appears and the solution becomes viscous. At this point, the rate of addition of sodium hydroxide should be slowed down and the total volume was adjusted to 500 ml. After adding sodium hydroxide solution, the reaction was allowed to continue for 5 h at room temperature (30 °C). The obtained mixture containing ZnO nano-particles is allowed to precipitate and separated by decantation. The mixture is filtered, washed twice with distilled water, dried at 100 °C and cured at 140 °C for 1 h. The obtained ZnO nano-particles is let to cool down in desiccators, and then kept in a stoppered bottle.

The nano-particles of ZnO were characterized by X-ray diffraction (XRD), transmission electron microscopy (TEM), and FT-IR spectroscopy techniques.

2.2.1.3. Synthesis of nano emulsion of water/GMA/acrylic acid. GMA and GMA/acrylic acid mixtures were emulsified using Egyptol (non-ionic detergent). GMA and acrylic acid are mixed with Egyptol (2–5 g) in a 1000 ml glass beaker. To that mixture, 450 ml of water at room temperature are added within 3 min. with continuous stirring using a strong homogenizer, and the stirring is continued for extra 10 min.

2.2.1.4. Synthesis of cellulose-g-GMA/AA. According to literature data (Navarro, Tatsumi, Sumi, & Matsumura, 2001; O'Connell, Birkinshaw, & O'Dwyer, 2006), cotton fabrics were first impregnated in a freshly prepared aqueous $FeSO_4(NH_4)2SO_4{\cdot}6H_2O$ (0.025%) for 20 min at 25 °C, using a fiber-to-liquor ratio of 1:50, then squeezed, washed thoroughly with distilled water and dried. About 8 g of ferrous-containing fabric is suspended in 400 ml nano-emulsion of GMA/water or GMA/AA/water under good stirring, where different ratios of GMA to Acrylic acid are used, in all experimental conditions the GMA or GMA/acrylic acid mixture represents 100% WOF. 0.05% of Hydrogen peroxide is added to the above suspension at room temperature. The grafting reaction is performed at 70 °C for 120 min, under nitrogen atmosphere. The homo-polymer is separated through soxhlet extraction with acetone for 24 h and dried at 60 °C until constant weight. Percent grafting (%G) was calculated as follows (Singh, Tiwari, Tripathi, & Sanghi, 2004):

$$\text{Grafting}\,(\%G) = \frac{W_1 - W_0}{W_1} \times 100$$

where W_1 and W_0, denote the weight of the grafted cellulose sample and the weight of the untreated cellulose sample, respectively.

2.2.2. Flame retardancy and water repellent treatments

Firstly, GMA or GMA/AA grafted cotton textiles are impregnated in a benzene solution containing different ratios of the equivalent amount to epoxy content from diethylphosphite.

The samples were passed through a laboratory padder giving a wet pick-up of 100%, repeat two times and the fabric is textiles were cured at 50 °C for 1 h.

These fabrics are coated with nano particles of zinc oxide and amino functionalized silica using pad-dry-cure method. Three suspended solutions of nano-ZnO and amino silica mixture were firstly prepared. The fabrics were immersed in suspended solutions of nano-ZnO/nano-aminated silica for 10 min. The fabrics are padded

in two dip and nip and then squeezed to a wet pick-up of 100%. Padded fabrics are dried at 80 °C for 10 min and then cured at 110 °C for 3 min. Cured fabrics were washed using 2 g/l of non-ionic detergent for 10 min in order to remove unbound nano-particles. Then the fabric was rinsed at least 10 times to completely remove all left soap residues.

2.3. Testes and analysis

2.3.1. Determination of amino group content on aminated silicon dioxide

A titration method was used to estimate the accessible amino group content of aminated silicon dioxide (Jagst, 2011; Jung, Moon, & Lee, 2012). Into a 125 ml flask, 0.1 g of aminated silicon dioxide and 25 ml of 0.01 M hydrochloric acid aqueous solution are added. The mixture is stirred at room temperature for 2 h, and then, the mixture is filtered and titrated with a standardized aqueous solution of sodium hydroxide using phenolphthalein as an indicator.

2.3.2. Determination of nitrogen content

Nitrogen content of the treated fabric was determined according to Kjeldahl method (Vogel, 1957).

2.3.3. Determination of Carboxyl content

The carboxyl content was determined by ASTM D1926-00 (ASTM Standard C33 (ASTM D1926-00), 2011).

2.3.4. Determination of the Epoxy Groups Content in grafted cellulose samples

The amount of available epoxy groups on the grafted cellulose samples is determined by pyridine–HCl method (Sidney, 1967). A known amount of cellulose sample (1 g) is refluxed for 20 min with 50 mL of pyridine–HCl mixture (2 mL HCl and 123 mL pyridine). After cooling down the solution, the amount of available epoxy groups was determined by titration of pyridine–HCl solution with 0.1 M NaOH.

2.3.5. Determination of the phosphorous content

30–60 mg of samples are burned in a modified oxygen-flask and phosphorous is determined spectrophotometrically as molybdenum blue (Belcher, Macdonald, Phang, & West, 1965).

2.3.6. Flammability test

The property of flame–retardancy was monitored according to the vertical burning test method (AATCC Test Method 34-1969) (AATCC Test Method (34-1969), 1972).

2.3.7. Determination of char yield (loss in weight)

The measuring of char yield is an appropriate factor for study the influence of flame retardancy (Chen et al., 2005; Gaan & Sun, 2007b). In this order, the weight of each sample before and after burning was measured and char yield was calculated according to following equation:

$$\text{Char yield} = \frac{W_2}{W_1} \times 100$$

where W_1, W_2 are weights of sample before and after burning, respectively.

2.3.8. Water repellent test

Water repellency was performed according to AATCC test method 22-1989 (spray test) (AATCC Test Method (22-2005), 2005).

2.3.9. Tensile strength, elongation at break and surface roughness of cotton fabrics

This test is carried out in the National Research Centre according to the ASTM Standard Test Method D-1682-1924 (ASTM Standard Test Method C33 (ASTM D-1682-1924), 2011) on a tensile strength apparatus type FMCW 500 (Veb Thuringer Industrie Werk Rauenstein 11/2612 Germany) at 25 °C and 65% relative humidity. The results quoted are the mean of 10 breaks for the warp direction with test length of 20 cm at a constant breaking time of 20 seconds load scale 10–50 kg.

Surface roughness was monitored according to JIS 94 standard, using surface roughness measuring instrument, SE 1700, made in Japan.

2.3.10. Fourier transform infra-red spectroscopy (FT-IR)

The FT-IR tester of Nicolet Magna-IR 560 spectrometer was used to analyze the spectrum of the treated and the untreated cellulose samples, CMS and CMS-ZnO nano-particles and amino functionalized silica. Resolution for the infrared spectra was 4 cm^{-1} and there were 32 scans for each spectrum. KBr was used to prepare the thin film together with the samples. The tester collected transmittance of the infrared in the film between 400 and 4000 cm^{-1}.

2.3.11. Scanning electron microscopy (SEM)

Scanning Electron Microscopy micro-analyzer (JXA-840A) Japan microscope S, at 15-kV acceleration voltage, after gold coating, was used to visualize Surface morphology of ungrafted and grafted cotton fabrics and the distribution of the polymer and particles coated the fiber surface.

2.3.12. Thermogravimetric and differential thermal analysis

Thermogravimetric (TGA) and differential thermal (DTA) analyses were performed with a Mettler-Toledo DTA/TGA instrument in the temperature range from 50 to 500 °C, at a rate of 10 °C/min, under nitrogen flow.

2.3.13. Transmission electron microscope (TEM)

Transmission electron microscope (TEM) observation was performed on a JEOL JEM-1230 electron microscope at accelerating voltage of 120 kV. Specimens for TEM measurements were prepared by depositing a drop of colloid solution on a 400 mesh copper grid coated by an amorphous carbon film and evaporating the solvent in air at room temperature. The average diameter of the aminated silica nano-particles and ZnO nano-particles was determined from the diameter of 100 nano-particles found in several chosen areas in enlarged microphotographs.

2.3.14. X-ray diffraction (XRD)

XRD patterns recorded of finely ZnO powdered, the untreated cotton, and the grafted cotton with GMA samples were recorded on a Philips PW 3050/10 model. The samples were recorded on a Philips X-Pert MMP diffractometer by monitoring the diffraction angle from 5° to 80° (2θ). The diffractometer was controlled an operated by a PC computer with the programs P Rofit and used a MoK (source with wavelength 0.70930 Å, operating with Mo-tube radiation at 50 kV and 40 mA.

The crystallinity of the sample (X_c, %) was calculated according to the following formula:

$$X_c(\%) = \frac{F_c}{F_c + F_a} \times 100$$

where F_c and F_a are the areas of crystalline and noncrystalline regions, respectively.

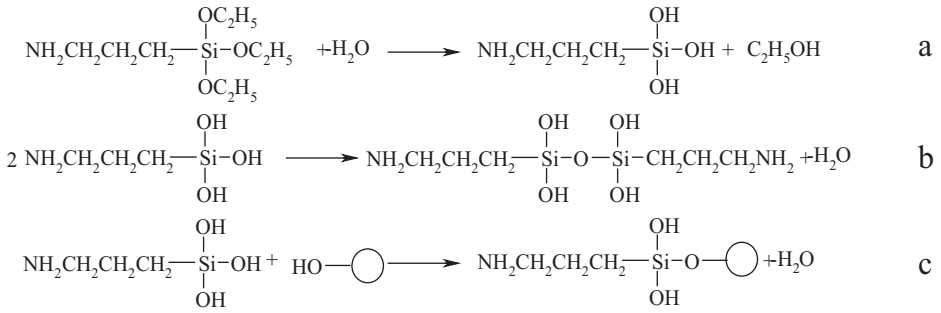

Fig. 1. Chemical equation of hydrolysis reaction from alkoxysilanes (a) and self-condensation reaction (b) or (c) condensation reaction between APTES and silica.

3. Results and discussions

The goal of this study is to investigate the suitability of silica nano-particles in combination with ZnO nano-particles to impart both flame retardancy and water repellency.

3.1. Preparation and characterization of aminated silica nano-particles

3.1.1. Introducing amino groups onto the silica surface

The treatment of silica with APTES resulted in silica particle containing amino groups on the surface, which acted as the initiator sites for other active polymers. The condensation reaction is base-catalyzed and APTES amine groups are self-catalyzed component. The mechanism involved the hydrolysis of APTES triethoxy groups by water, yielding silanol groups. Then condensation reaction between APTES silanol group and silica silanol group took place on silica surface as shown in Fig. 1. The amount of water present in the system significantly influenced the hydrolysis reaction of triethoxy groups and the condensation reaction on silica surface (Simon, Cohen-Bouhacina, Porté, Aimé, & Baquey, 2002).

The rate of hydrolysis and condensation reaction was controlled by using a mixture of water and methanol (Arkles, Steinmetz, Zazyczny, & Mehta, 1992; Punyacharoennon, Charuchinda, & Srikulkit, 2010; Stober, Fink, & Bohn, 1968). In this study, the methanol to water ratio 2:1 was used. Water was consumed to convert APTES triethoxy groups into silanol groups (hydrolysis reaction). The amount of water, hence, determined the rate of hydrolysis. Consequently, the more silanol groups produced the higher the rate of subsequent silanol condensation reaction (Punyacharoennon et al., 2010; Stober et al., 1968). Amino-functionalized silica for active cellulose grafting was prepared as follows: a 2:1 ratio of methanol to water was used and the surface functionalization of silica particles was allowed to take place for three days.

Amino group content of amino grafted silicon dioxide was determined as 5 mmol/g, while nitrogen content was determined as 6%.

Fig. 2 compares FT-IR spectra between APTES grafted silicon dioxide, virgin silicon dioxide and APTES. Silicon dioxide which is an inorganic substance in nature exhibits the strong absorption band of siloxane (Si—O—Si) bonding at ~1200 cm^{-1} and the silanol OH band in the range of 3200–3400 cm^{-1}. When considering the APTES silicon dioxide, organo-functionalized silica, its spectrum exhibits new absorption frequencies at 2932 and 1640 cm^{-1}. These bands are associated to C—H stretching and primary amine ($-NH_2$) stretching absorptions, respectively. In addition, these bands are found corresponding with the absorption characteristics of APTES spectrum. These results indicate that APTES was incorporated into silicon dioxide particles. The silica surface modification is further confirmed by change observed in spectrum pattern in the region of silanol OH band (3200–3400 cm^{-1}) due to new inter-hydrogen bonding interaction among APTES silicon dioxide particles.

Fig. 3 shows TEM of amino functionalized nano-particles micrographs. It is clear from the micrographs that amino functionalized silica nanoparticles exhibit round shapes. The high agglomeration of the small size particles had been shown in TEM micrographs. Calculation of the particle size of amino functionalized silica had been done using Revolution TM V1.6 0b 195 software, for the ten micrographs at different areas, it was found that particle size is in the range of 15–25 nm.

Fig. 3 illustrates the size distribution of amino functionalized silica, the distribution curves indicate that the particles size ranging from 35 to 5 nm (most of them between 15 and 20 nm).

3.2. Characterization of ZnO nano-particles

3.2.1. FT-IR spectra of CMS and CMS-ZnO nanoparticles

Fig. 4 shows the FT-IR spectra of both CMS and CMS-ZnO nano-particles. The FT-IR spectra of CMS show bands at 3413, 2927, 1603 and 1013 cm^{-1} characteristic for hydrogen stretching of bonded O—H, hydrogen stretching of C—H, double bond stretching of carbonyl, carboxyl, carboxyl salt, and hydrogen bending of O—H respectively with corresponding intensities of 73, 79, 76 and 69%T, respectively. Same characteristic bands for CMS-ZnO nanoparticles appeared at 3350, 2927, 1592 and 1024 cm^{-1} at either the same frequencies (2927 cm^{-1}) or with little shift to different frequencies (3350, 1592 and 1024 cm^{-1}). The strengths of the bands of CMS-ZnO nano-particles (64, 71, 69 and 65%T, respectively) are completely different from CMS. These observations confirm the

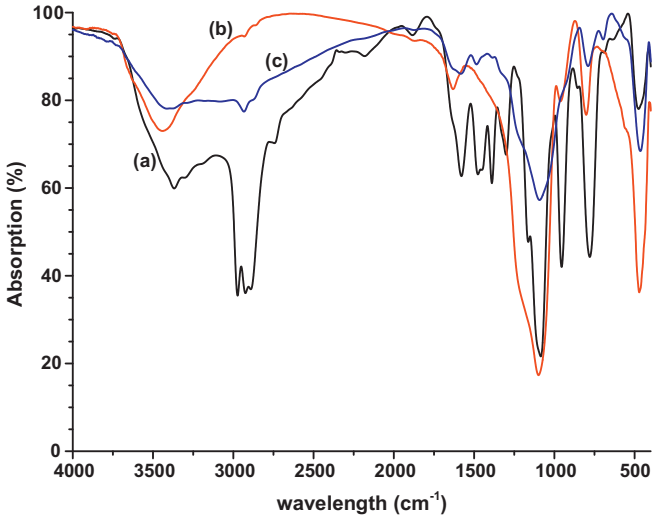

Fig. 2. FT-IR spectra of (a) APTES, (b) virgin silicon dioxide and (c) APTES.

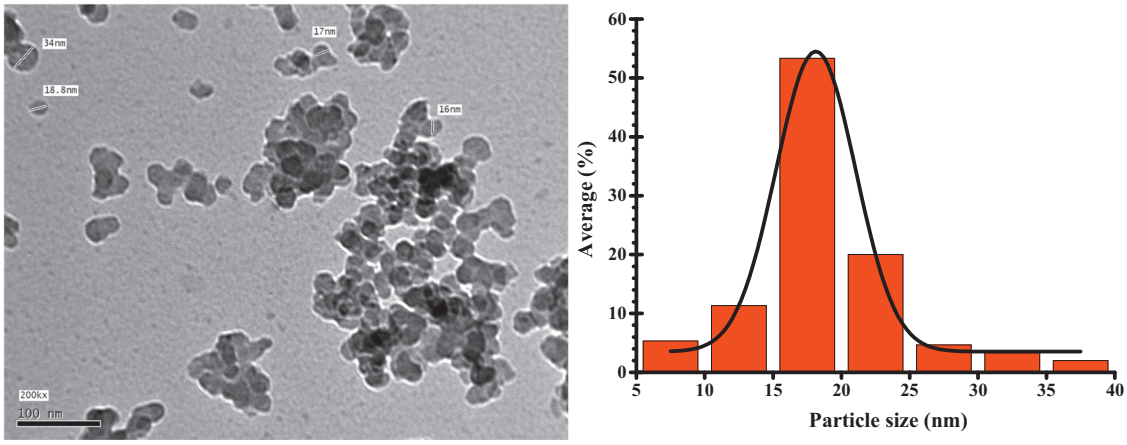

Fig. 3. TEM and size distribution of amino functionalized silicon.

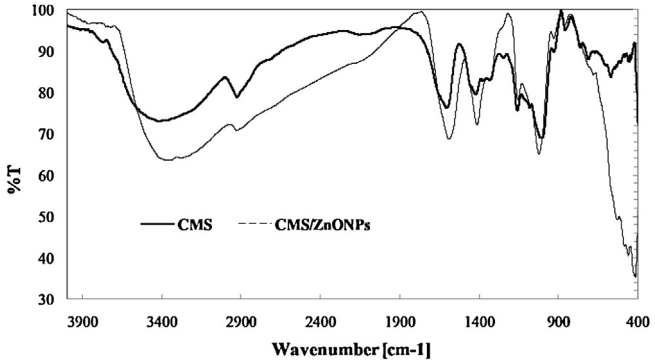

Fig. 4. FT-IR spectra of CMS and CMS-ZnO nano-particles.

interaction of the carbonyl, carboxyl or carboxyl salt and the OH groups in the synthesis and stabilization of ZnO nano-particles. The appearance of a dominant ZnO absorption bands between 400 and 480 cm^{-1} corresponding to the two transverse optical stretching modes of ZnO (Anžlovar, Orel, & Žigon, 2010; Kathirvelu, D'Souza, & Dhurai, 2009).

3.2.2. TEM of CMS-ZnO nanoparticles

Fig. 5 shows TEM of two CMS-ZnO nano-particles micrographs. It is clear from the micrographs that ZnO NPs exhibit both round and rod shapes. Aggregations of ZnO NPs were also seen. By calculating the size of ZnO NPs using Revolution TM V1.6 0b 195 software, for the two micrographs at different areas, it was found that particle size is in the range of 10–69 nm.

3.2.3. XRD of CMS and CMS-ZnO nanoparticles

Fig. 6 shows the XRD of CMS and CMS-ZnO nano-particles respectively. Fig. 6a shows three strong characteristic peaks at 14.87°, 17.37° and 22.85° characteristic to CMS. These peaks were totally disappeared in case of CMS-ZnO NPs. On the other hand, XRD diffractograms of the synthesized ZnO (Fig. 6b) show well-defined peaks typical to ZnO in the crystal structure of zincite this indicates crystallinity of the synthesized solid. XRD spectra of the synthesized ZnO (Fig. 6b) show also broad peaks at 31.7; 34.4; 36.2; 47.5; 56.6; 62.8; 66.3; 67.9; 69; 72.6 and 77 (Fig. 6b) which are typical for the hexagonal ZnO wurtzite structure. Rather broad diffraction peaks indicate the small size of crystallites (Anžlovar et al., 2010; Kathirvelu et al., 2009).

3.3. Characterization of nano emulsion of water/GMA/acrylic acid

TEM analysis was used to investigate the particle size of the GMA and GMA\AA nano-emulsion. Fig. 7 shows TEM micrograph of the prepared emulsion, it is illustrated the small size particle of GMA and GMA\AA. No agglomeration of the small size particles had been shown in TEM micrographs. Calculation of the particle size of the prepared emulsions had been done using Revolution TM V1.6 0b 195. It is clear that the particle size of GMA/water emulsion is smaller than GMA/AA/water emulsion, where the particles are in the range of (35–70 nm) and (40–95 nm) for GMA and GMA/AA respectively.

3.4. Synthesis and characterization of GMA/acrylic acid grafted cellulose (GMA-C)

Cellulose can be functionalized by grafting several vinyl monomers to polymeric chains to obtain the modified celluloses. cell-g-GMA\AA was synthesized through graft copolymerization reaction using cotton cellulose with nano-emulsion consisting of mixture of GMA and acrylic acid with different ratios.

The presence of acrylic acid in the system will create an interpenetrating polymer network with free COOH groups at the chain end in addition of the free epoxy group of glycidyl methacrylate The acidic groups like COOH in the chain will help to attach the ZnO in the polymer network. Table 1 shows the epoxy content, the carboxyl content and the grafting% (G%) of the grafted cotton fabrics, it is illustrated that, with the increase of the grafting percentage, the epoxy content rise from 4.3 to 5.2 mmol/g and the carboxyl content rise from 0.52 to 1.8 mmol/g. At first, grafting occurred onto the fiber surface, mostly in the amorphous region (Yang & Zhai, 2012). With increasing of the GMA monomer, it was onto the fiber backbone and G% increased. The polar hydroxyl groups were replaced by the non-polar ester (also epoxy group) bond on the surface, which resulted in the increase of the epoxy groups and water repallancy (Chruściel & Leśniak, 2012). However, a too much grafted GMA did not bring the value of the contact angle to a higher level, causing the destruction of the crystalline region instead (according to the results of XRD analysis), which was not beneficial to the surface non-polarity and construction of the treated fabrics.

Reaction mechanism of grafting of AA and GMA onto cellulose is divided into 3 steps:

Initiation reactions

$$Fe^{2+} + H_2O_2 \rightarrow Fe^{3+} + HO^- + HO^\bullet$$

$$\text{Cell-OH} + HO^\bullet \rightarrow \text{Cell-O}^\bullet + H_2O$$

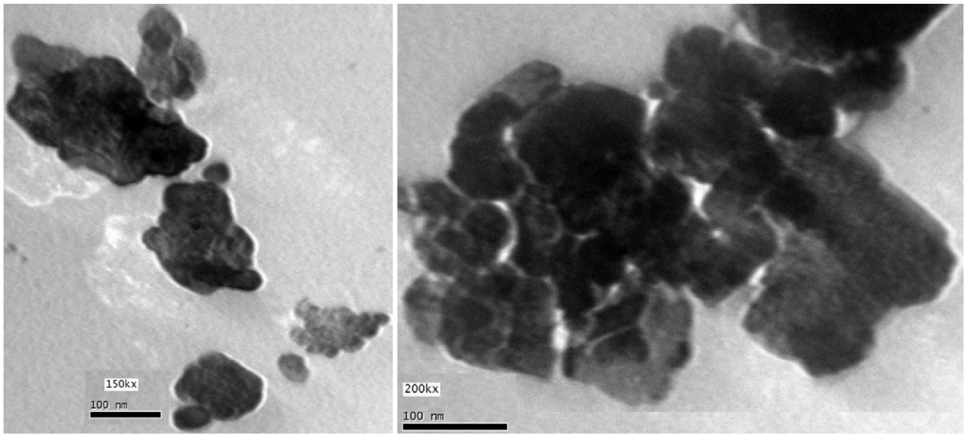

Fig. 5. TEM of CMS-ZnO nano-particles.

GMA and AA + 2HO• → AA• and GMA•

First, the Fenton-redox reaction dissociates the hydrogen peroxide generating a hydroxyl ion and one OH• radical. This very reactive radical will immediately react with whatever is available, either cellulose or monomer. Cellulose macro-radicals are formed by the abstraction of an H-atom, probably from one of the hydroxyl groups. But when the OH radical meets a monomer molecule first, it will also react rapidly, opening up the vinyl bond. So, both grafting and homopolymerization will be initiated at the same time.

The primarily formed cellulose radical reacts with AA and/or GMA, which may also be regarded as an initiation step:

Cell• + AA or GMA → Cell-g-AA• or Cell-g-GMA•

Further propagation reactions

Cell-g-AA• + AA → Cell-g-(AA)2•

→ Cell-g-(AA)n• (main reaction-grafting)

or

Cell-g-GMA• + GMA → Cell-g-(GMA)2•

→ Cell-g-(GMA)n• (main reaction-grafting)

Termination reactions

Cell-g-(AA)n• + Cell-g-(GMA)m• → Cell-g-(AA)n-Cell-g-(GMA)m

or

Cell-g-(GMA)n• + (AA)m• → Cell-g-(GMA)n-(AA)m

3.4.1. FT-IR spectroscopy

FT-IR spectroscopy is a common technique used to investigate the structural changes of cellulosic material upon chemical reactions. Fig. 8 shows the FT-IR spectra profiles of untreated cellulose and of the three grafted cellulose-g-GMA\AA samples. The FT-IR spectrum of untreated cotton presents the bands typical of cellulose: 3400 cm^{-1} (O—H stretching); 2910 cm^{-1} (C—H stretching); 1640 cm^{-1} (absorbed water); 1430 cm^{-1} (CH2 bending); 1380 cm^{-1} (O—H bending); 1320 cm^{-1} (C—C and C—O vibrations); 1220–920 cm^{-1} (C—O asymmetric bridge stretching and C—O—C pyranose ring skeletal vibrations); 895 cm^{-1} (β-glycosidic linkage) (Shukla & Athalye, 1994). The comparison between the FT-IR spectra of cotton cellulose and of cellulose grafted derivatives

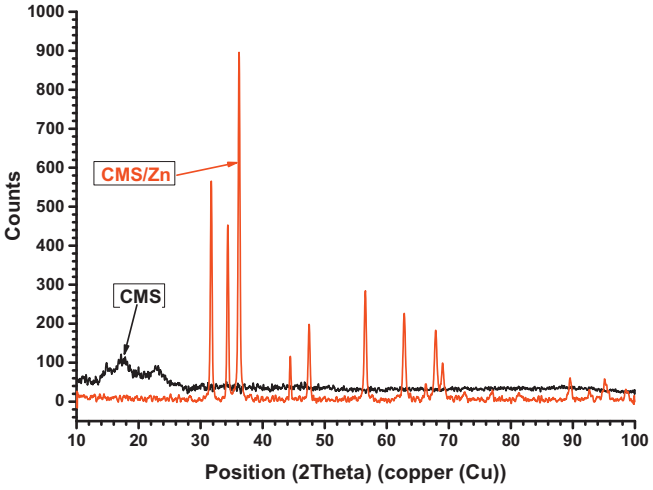

Fig. 6. XRD of (a) CMS and (b) CMS-ZnO nanoparticles.

demonstrates the functionalization of the glucose units, since several additional peaks were found for cellulose grafted derivatives, compared to the untreated cellulose. The peak at 1733 cm^{-1} should be assigned to the >C=O stretching vibration, indicating the presence of an ester group of GMA and or AA grafted cellulose. The characteristic adsorption peaks at 906 cm^{-1} (asymmetrical stretching vibration of the epoxy group) and 1710.74 cm^{-1} (—COOH) group which is due to the introduction of acrylic acid graft onto the cellulose Skelton. Which evidence that grafting of GMA onto fibers had occurred. The peak intensity at about 3000 cm^{-1}, corresponding to the C–H stretching vibration of the epoxy group, increased obviously, when GMA% increased.

3.4.2. XRD analysis

Fig. 9 shows the XRD (X-ray diffraction) patterns of cotton fibers and grafted fibers, and it is shown that, a wider peak with low intensity was observed at around $2\theta = 22.48^{\circ}$. The crystallinity of cotton fiber and the grafted cellulose with GMA/AA nano emulsion value (G% = 217.1%) was of 69.8 and 36.5%, respectively. The decrease in crystallinity after grafting should be attributed to the randomness of the amorphous phase in the graft copolymers enhanced by grafting with GMA, which caused perturbation of the long-ranged spacing between chains (Wang et al., 2009).

Table 1
Grafting yield, epoxy and carboxyl content of treated cotton fabrics.

Sample name	Label	GMA:AA ratio	Epoxy content (mmol/g)	Carboxyl content (mmol/g)	G%
Cell-g-GMA/AA_1	Cg1	90:10	4.3	0.52	95
Cell-g-GMA/AA_2	Cg2	80:20	3.6	1.20	92
Cell-g-GMA/AA_3	Cg3	70:30	2.8	1.80	90
Cell-g-GMA	Cg4	100:0	5.2	0	100

GMA: glycidyl methacrylate AA: acrylic acid G%: grafting yield.

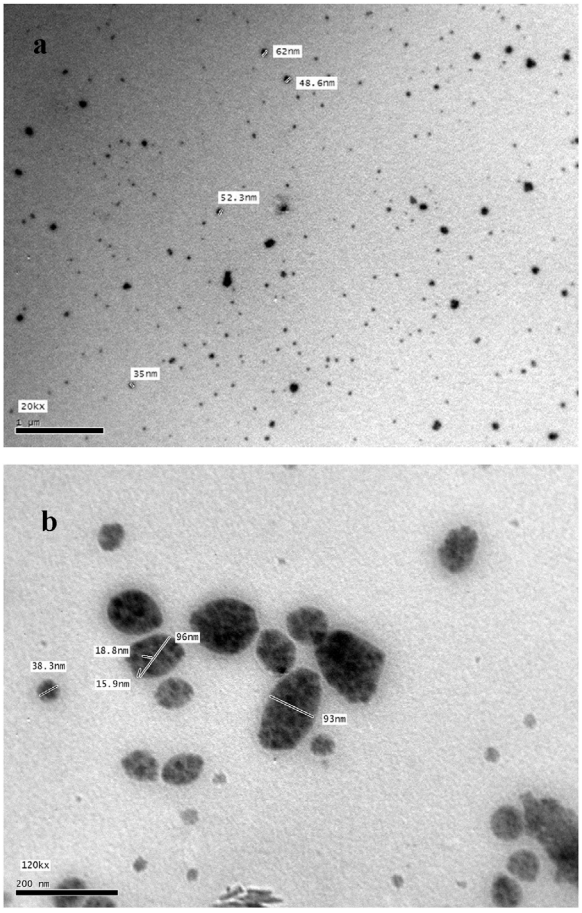

Fig. 7. TEM micrograph of the prepared emulsion of (a) GMA and GMA/AA and (b) GMA/water.

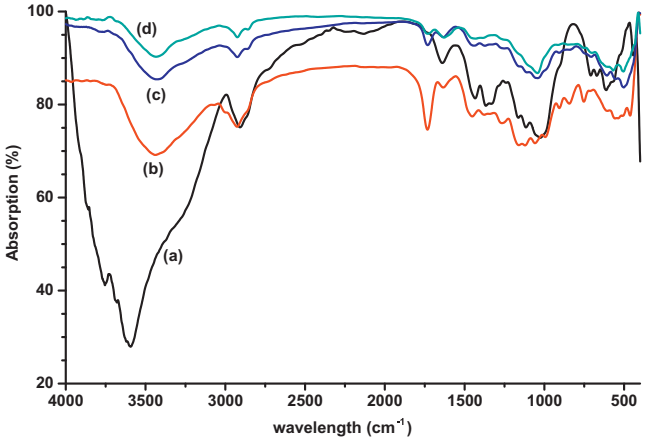

Fig. 8. FT-IR spectra profiles of (a) untreated cellulose, (b) grafted cellulose-g-GMA\AA (1), (c) grafted cellulose-g-GMA\AA (2) and (d) grafted cellulose-g-GMA\AA (4) samples.

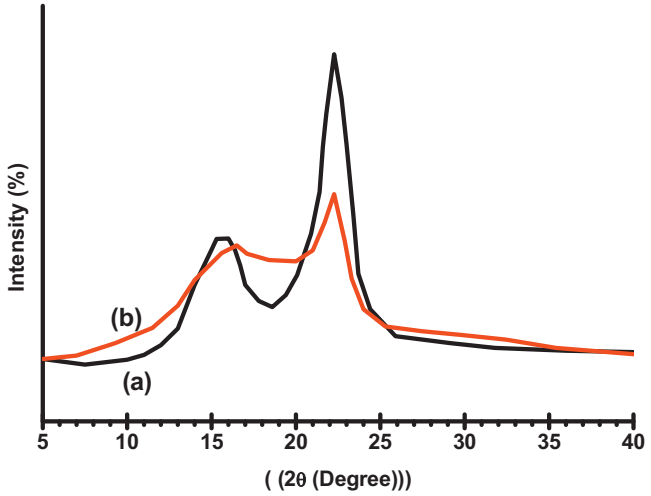

Fig. 9. XRD (X-ray diffraction) patterns of (a) cotton fibers and (b) grafted fibers.

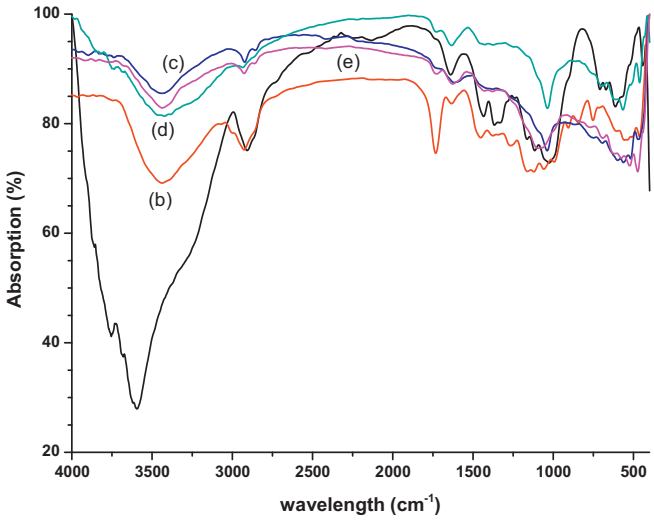

Fig. 10. FT-IR spectra of pure cotton and treated cotton fabrics at different treatment condition.

3.5. Characterization of functional textiles

3.5.1. FT-IR analysis

Spectrum of pure cotton (Fig. 10) exhibited O—H stretching absorption around 3440 cm^{-1}, C—H stretching absorption around 2800–3000 cm^{-1}, and C—O—C stretching absorption around 1056 $cm^{-1}$and 1110 cm^{-1}. These absorptions are consistent with those of the typical cellulose backbone. After modification with GMA/AA, the peak intensities at 2920 cm^{-1} and 1060 cm^{-1} increase obviously, which is attributed to the introduction of the $-CH_2$groupsand the peak intensity at 1280 cm^{-1} increases slightly due to the introduction of the epoxy rings. After silica coating and ZnO, a new peak at 2850 cm^{-1} appears in the spectrum of sample

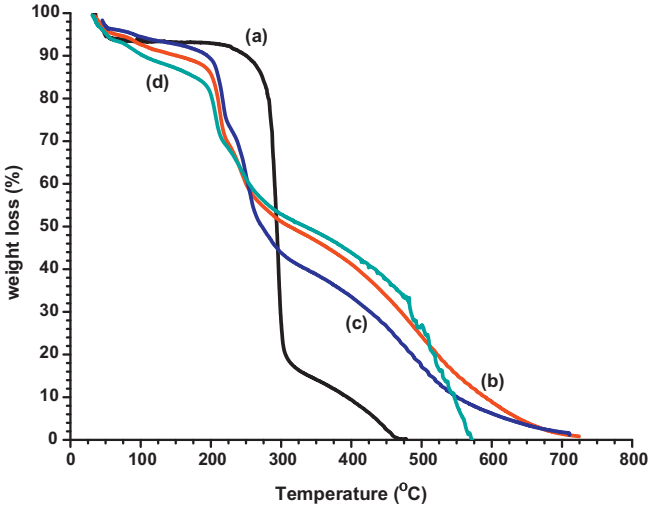

Fig. 11. TGA curves of (a) untreated, (b) treated cotton fabrics.

A3, and increased peak intensity is observed at 2920 cm^{-1} of —CH_2 due to C-symmetric and anti-symmetric stretching, respectively. In addition, the peak intensity at 1110 cm^{-1} is strengthened very much and becomes stronger than that at 1060 cm^{-1}, which is as a result of the introduction of Si—O—Si since the peak intensity at 1110 cm^{-1} is less strong than that at 1060 cm^{-1} in the spectra of pure cotton and epoxy-functionalized cotton. The oscillating spectra of silica are characterized by additional bands, which distinguish them from mono- and disilicates (Si—O—Si in the similar region of 600–800 cm^{-1}) (Mohamed, Er-Rafik & Moller, 2013a, 2013b). In the modified fibers, the symmetric stretching vibration of Si—O—Si was found, which is specific for cyclosilicates, at a wave number of 759 cm^{-1} and, to a lesser degree, 719 cm^{-1}. The modified cellulose with amino silica spectrum is flattened mostly in the region characterized by the presence of the strongest absorption bands of skeletal silicates including SiO_2 and its polymorphic versions. The partial overlapping in the region of absorption bands that is characteristic for both cellulose and silicates makes identification rather ambiguous; the asymmetric stretching vibration of —C—O—C— (1164 cm^{-1}, cellulose) and the asymmetric stretching vibration of —Si—O—Si— (1171 cm^{-1}, silicates) being examples. The FT-IR analysis of Cell/Si fibers did not reveal —Si—O—C— or Si—C bonds, which would witness the existence of chemical bonds between the portion of silicates and the cellulose chains.

3.5.2. Thermal analysis of cell-g-poly(GMA)

Fig. 11 illustrates TGA thermograms of pure cellulose, grafted cellulose diethylphosphite, amino-functionalized silica and ZnO nano-particles shown in Fig. 11 presents the decomposition temperature of treated and untreated cotton fabrics. The untreated fabric starts to decompose at about 3000 C, continues to reach the 100% weight loss at 350 °C (Zhu, Sui, Wang, Sun, & Sun, 2004). It is found that, grafted cotton textiles lose all their weight after being heated to 550 °C, indicating all the substances are burned away.

In case of treated fabrics, the temperature of degradation begins at the relatively lower temperature of 290 °C. The pyrolysis of flame retardant finished cotton fabric has lower decomposition temperature because of a catalytic dehydration of cellulose by the flame retardant, leading to char forming on fabric surface. The decline of degradation temperature is because the phosphorous compounds react with C6 hydroxyl of the cellulose anhydroglucose unit, blocking the formation of levoglucosan (source of fuel). Then, it will reduce the amount of fuel to the flame and promote char formation. Moreover, its structure contains nitrogen atoms which act synergistically with phosphorus (Gaan & Sun, 2007a). It is known that nitrogen enhances the electrophilicity of phosphorous thereby making a stronger Lewis acid and also promoting the phosphorylation reaction with C(6) hydroxyl group of anhydroglucose unit.

Samples coated by amino-functionalized silica particles, lose about 96.3% of their weight, as shown in Fig. 11. The remaining weight about 3.7% is attributed to the residue of SiO_2, indicating the coated of silica to the fiber surfaces. The treatment of cotton fabrics with nano-sized ZnO does not modify significantly their thermal stability and maximum pyrolysis temperature (Becheri, Dürr, Lo Nostro, & Baglioni, 2008).

3.5.3. SEM analysis

Morphological investigation of the pure cotton and GMA/AA-grafted cotton fibers, which coated with silica and ZnO nanoparticles, was conducted with a scanning electron microscope (SEM), the recorded images being shown in Fig. 12. The smoothness and evenness of the fiber surface were observed on the original fiber. The changes in surface morphology after grafting with GMA/AA and coated clearly revealed that grafting affected the cotton fiber surface. Surface unevenness resulted from polymer deposition during graft copolymerization and the loaded silica and ZnO, which deposited and dispersed on the fiber surface. In addition, the grafted cotton fiber was plumper than the original one, which might be caused by excessive grafting, affecting the fiber inner lumen wall.

3.5.4. Grafting yield, epoxy and carboxyl content

Table 1 shows the grafting yield, the epoxy and the carboxyl content of the grafted cotton fabrics, from this table it is clear that, by increasing the concentration of GMA related to the concentration of the AA in the grafting process the epoxy content increased. In opposite direction the carboxyl content increased by increasing the concentration of AA related to the concentration of the GMA in the grafting mixture. Meanwhile, with the increase of the grafting percentage, the epoxy content rose from 2.8 to 5.2 mmol/g. At first, grafting occurred onto the fiber surface, mostly in the amorphous region. With increasing of the GMA monomer, it was grafted onto the fiber backbone and G% increased. In general, the grafting yield increased by increasing the content of GMA in the grafting bath.

3.5.5. Nitrogen and phosphorus content

Table 2 shows the nitrogen and phosphorus content of the treated cotton fabrics, from this table it is clear that, by increasing the concentration of GMA related to the concentration of the AA in the grafting process the nitrogen content and Phosphorus increased. That is attributed to the increase of available epoxy groups, which are capable of binding via covalent bonding with both amino group of amino functionalized silica as well as the phosphite group of the diethyl phosphite. By increasing the amount of reacted silica the nitrogen content of the treated fabrics increased. On the other hand, increasing the amount of reacted diethyl phosphate causes significant increase for phosphorus of the treated fabrics.

3.5.6. Flammability test of the treated fabric

As already demonstrated, that incorporation of silicon and silica particles to the finishing formula is a useful method to enhance the flame retardancy of synthetic and natural textile substrates. The presence of the silica coating onto the textile surface modifies the combustion behavior of cotton by decreasing the total heat release, the mass loss rate and, consequently, the effective heat of combustion. This finding points out that the silica coating is able to protect the polymer from oxygen and heat transfer, blocking its decomposition. The silica coating is also able to delay the ignition of the sample (Alongi, Ciobanu, & Malucelli, 2011).

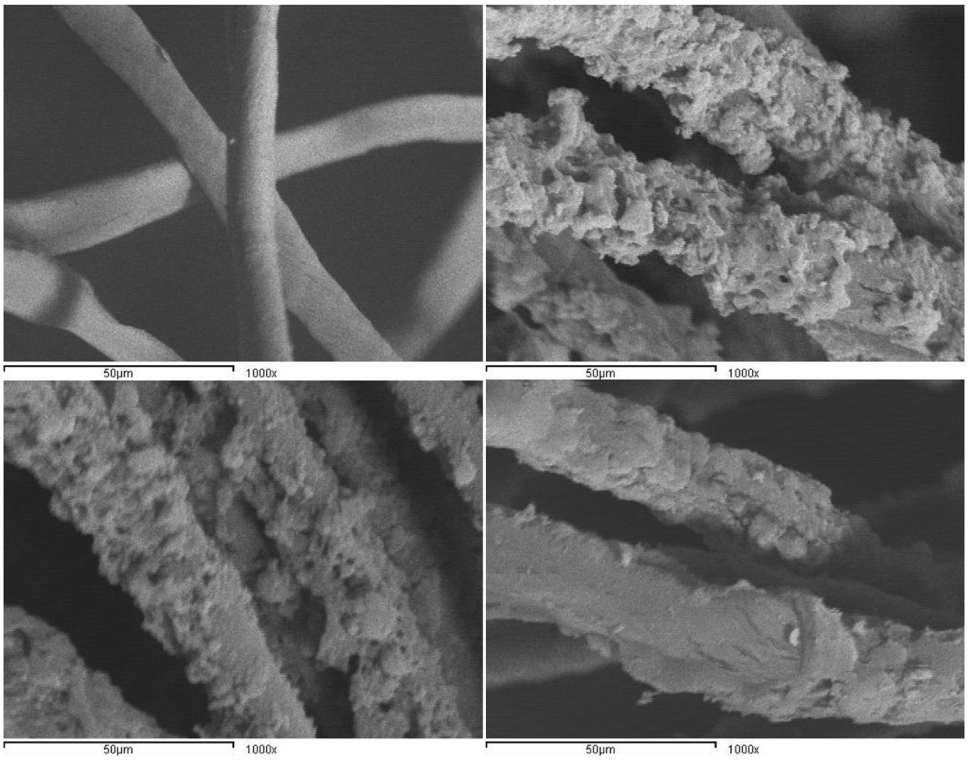

Fig. 12. SEM micrograph of untreated and treated cotton fibers.

Incorporation of diethyl phosphite with amino functionalized silica potentially offered powerful chelating action and flame retardancy properties. In the treatment of cotton, it was expected to render cotton fire resistant. The treated cotton fabric was subject to vertical burning test. Its burning behavior was compared with those of untreated cotton.

Table 2 shows the effect of incorporation of organo phosphorus compound with both silica and ZnO nano-particles in the same finishing formulation on the flame retardant properties of finished cotton fabrics.

The results signify that at any of the finishing formulae there is an improvement in the flame retardancy properties, where, all the treated fabrics are non-flammable, while increasing the ratio of phosphorus compound brings high phosphorus content of the treated cotton fabrics. The results in Table 2 reveal also that the flame retardancy in presence or in absence of ZnO is good. The presence of both nitrogen and phosphorous, leads to the prevention of levoglucosan formation and reduce the flammability of the finished cotton fabric. The presence of silica and ZnO nanoparticles enhances the flame retardant property of the treated fabrics.

Table 2
Physical properties of treated fabric.

	Diethylphosphite:aminated SiO_2:ZnO	Label	Flammability			Nitrogen (%)	Phosphorus (%)
			Loss in weight (%)	Area of chaired zone (cm^2)	Chair length (cm)		
0	0	0					
	0.75:0.25:1.2	Cg1_1	3.8	1.24	0.03	1.3	1.2
	0.50:0.50:1.2	Cg1_2	3.9	1.55	0.25	2.5	0.9
Cg1	0.25:0.75:1.2	Cg1_3	4.0	2.09	0.29	3.5	0.5
	1:0:1.2	Cg1_4	5.7	2.40	1.40	0	1.5
	0:1:1.2	Cg1_5	8.0	3.63	2.00	5	0
	0.75:0.25:1.2	Cg2_1	4.0	2.16	0.29	1.1	1.1
	0.50:0.50:1.2	Cg2_2	5.0	2.00	1.40	2.2	0.8
Cg2	0.25:0.75:1.2	Cg2_3	5.5	2.24	1.50	3.1	0.4
	1:0:1.2	Cg2_4	6.0	2.40	1.80	0	1.2
	0:1:1.2	Cg2_5	6.5	2.65	2.00	4.3	0
	0.75:0.25:1.2	Cg3_1	4.0	2.10	0.30	0.75	0.92
	0.50:0.50:1.2	Cg3_2	4.5	2.16	0.32	2	0.65
Cg3	0.25:0.75:1.2	Cg3_3	5.0	2.20	1.30	2.8	0.2
	1:0:1.2	Cg3_4	5.5	2.50	1.30	0	1.1
	0:1:1.2	Cg3_5	6.5	2.70	1.90	4	0
	0.75:0.25:0	Cg4_1	7.0	2.90	3.00	1.5	1.5
	0.50:0.50:0	Cg4_2	8.0	3.26	3.50	2.8	1.2
Cg4	0.25:0.75:0	Cg4_3	9.5	3.65	3.50	4	0.7
	1:0:0	Cg4_4	10.6	3.90	3.70	0	1.8
	0:1:0	Cg4_5	11.0	4.50	4.00	5.6	0

Table 3
Mechanical properties and water/oil repellancy of treated fabric.

	Diethylphosphite:aminated SiO_2:ZnO	Label	Mechanical properties			Water repellency WRR
			TS (kg)	El (%)	Roughness (μm)	
0	0	0	41	15	17.65	20
	0.75:0.25:1.2	Cg1_1	37.5	13.63	19.59	80
	0.50:0.50:1.2	Cg1_2	37.2	13.2	18.90	90
Cg1	0.25:0.75:1.2	Cg1_3	38.6	14.5	17.90	90
	1:0:1.2	Cg1_4	36.7	11.7	18.90	70
	0:1:1.2	Cg1_5	37.5	12.8	17.50	100
	0.75:0.25:1.2	Cg2_1	38.6	13.6	20.60	80
	0.50:0.50:1.2	Cg2_2	38.9	13.2	19.90	90
Cg2	0.25:0.75:1.2	Cg2_3	39.1	14.1	18.20	100
	1:0:1.2	Cg2_4	37.5	12.4	19.90	80
	0:1:1.2	Cg2_5	39.0	14.1	17.60	100
	0.75:0.25:1.2	Cg3_1	38.9	13.6	22.70	70
	0.50:0.50:1.2	Cg3_2	38.7	13.6	21.90	80
Cg3	0.25:0.75:1.2	Cg3_3	39.2	14.2	19.10	90
	1:0:1.2	Cg3_4	37.1	12.6	22.90	80
	0:1:1.2	Cg3_5	39.3	14.5	18.90	100
	0.75:0.25:0	Cg4_1	33.0	10.6	18.90	60
	0.50:0.50:0	Cg4_2	34.7	11.5	18.20	70
Cg4	0.25:0.75:0	Cg4_3	35.7	11.75	17.90	80
	1:0:0	Cg4_4	31.5	10.11	19.20	30
	0:1:0	Cg4_5	39.2	13.69	17.90	90

3.5.7. *Water repellency tests*

Evaluation of fabric hydrophobicity is difficult to assess by any one method. The drop test enables a quick and easy determination, while multiple methods of testing help us to know performance and quality of the material more precisely. To ascertain the water-repellency characteristics of the fabric, the resistance of the fabric to surface penetration by a spray and resistance to surface wetting should be measured. Tests have to be carried out in combination with each other in order to obtain a complete understanding of performance. Samples were assessed for performance using drop test, spray test and contact angle measurement.

Grafted cotton modified with amino silicon and ZnO nanoparticles displayed drop test results greater than 30 min. In fact, superhydrophobic character was found with all treated samples with the mixture amino silicon and ZnO nanoparticles, all of which displayed strong hydrophobic character.

Water repellency (WRR) in Table 3 showed that growth of ZnO nano-particles on fibers further increased the superhydrophobicity due to the surface roughening effect, as evidenced by SEM in Fig. 12. Coating of SiO_2 on the textiles might slightly decrease the roughness of the ZnO nano-particles decorated textiles, thus showing a slight decrease of the corresponding WRR.

3.5.8. *Mechanical characterization*

Table 3 illustrates the mechanical and physical properties of untreated and treated cotton fabrics. The results in Table 3 indicate that the finishing treatment is accompanied by a significant decrease in tensile strength and elongation at a break of the treated fabrics. On the other hand, the treatment leads to slight increase in roughness values. This is observed irrespective of the substrate used. This may be due to the deposition of nanoparticles of ZnO on the treated cotton. The grafting process also, causes the increase of roughness, decreases the tensile strength and the elongation at a break.

4. Conclusion

Nanoparticles of ZnO and amino functionalized silica have been prepared using new techniques in order to functional finished cotton fabrics to produce technical textile with high performance, regarding the environmental aspect. Cotton cellulose had been activated via grafting copolymerization of GMA/AA into the cellulose backbone, in order to facilitate the reaction between cellulose and nanoparticles. A novel flame retardant system consisted of diethyl phosphite in combination with the two mentioned nanoparticles had been investigated. The characterizations of the treated fabrics indicate the new chemical structure of the treated fabrics.

The performed treatment helps to form more non-flammable char residue and increases char formation after heating in addition to the improvement of the water repellency property. Nano ZnO was investigated as a novel flame retardant for cotton and fabrics. Some analyses including char length, char yield and SEM in addition to the physical properties of the treated fabrics were studied in order to evaluate flame retardant property of treated samples. Nano ZnO is an effective compound in decreasing the flammability of the treated fabrics. In addition, the presence of phosphorus deposited on the diethyl phosphite treated samples is the most effective parameter in the char forming and decreasing the flammability of the treated fabrics.

Superhydrophobic surfaces on cotton textiles have been prepared. The epoxy- and carboxyl functionalization of the cotton enhances the interaction between the fiber and the silica coating and ZnO coating. The incorporation of the functionalized SiO_2 particles not only generates a firm dual-size rough surface but also facilitates the further hydrophobization of the surface.

The achieved coating surfaces are robust and the superhydrophobicity of the cotton textile is lasting. This strategy based on traditional textile treatment method might help to advance the large-scale area fabrication of superhydrophobic surfaces on flexible substrates.

Acknowledgement

This work was financial supported by National Research Center, Cairo, Egypt, with Project No. P90301/2012-2013

References

AATCC Test Method (22-2005). (2005). *Water repellency: Spray test. Institution, Year, Title, Publisher, Place Published, Year, doi: DOI, URL.* USA: Technical Manual Method of the American Association of Textile Chemists and Colorists.

AATCC Test Method (34-1969). (1972). *Vertical burning test method in fire resistance of textile fabrics. Technical manual method* (vol. 48) USA: Technical Manual Method of the American Association of Textile Chemists and Colorists.
Abidi, N., Hequet, E., & Tarimala, S. (2007). Functionalization of cotton fabric with vinyltrimethoxysilane. *Textile Research Journal*, *77*(9), 668–674.
Alongi, J., Ciobanu, M., & Malucelli, G. (2011). Novel flame retardant finishing systems for cotton fabrics based on phosphorus-containing compounds and silica derived from sol–gel processes. *Carbohydrate Polymers*, *85*(3), 599–608.
Annakutty, K. S., & Kishore, K. (1988a). Flame retardant polyphosphate esters: 1. Condensation polymers of bisphenols with aryl phosphorodichloridates: Synthesis, characterization and thermal studies. *Polymer*, *29*(4), 756–761.
Annakutty, K. S., & Kishore, K. (1988b). A novel approach to structure—flammability correlation in polyphosphate esters. *Polymer*, *29*(7), 1273–1276.
Anžlovar, A., Orel, Z. C., & Žigon, M. (2010). Poly(methyl methacrylate) composites prepared by in situ polymerization using organophillic nano-to-submicrometer zinc oxide particles. *European Polymer Journal*, *46*(6), 1216–1224.
Arkles, B., Steinmetz, J. R., Zazyczny, J., & Mehta, P. (1992). Factors contributing to the stability of alkoxysilanes in aqueous solution. In K. L. Mittal (Ed.), *Silanes and other coupling agents* (pp. 91–104). Netherlands: Utrecht.
ASTM Standard C33 (ASTM D1926-00). (2011). *Standard test methods for carboxyl content of cellulose. Institution, Year, Title, Publisher, Place Published, Year, doi: DOI, URL*. West Conshohocken, PA: ASTM International.
ASTM Standard Test Method C33 (ASTM D-1682-1924). (2011). *Standard test methods for institution, year, title, publisher, place published, year, doi: DOI, URL*. West Conshohocken, PA: ASTM International.
Banks, M., Ebdon, J. R., & Johnson, M. (1994). The flame-retardant effect of diethyl vinyl phosphonate in copolymers with styrene, methyl methacrylate, acrylonitrile and acrylamide. *Polymer*, *35*(16), 3470–3473.
Becheri, A., Dürr, M., Lo Nostro, P., & Baglioni, P. (2008). Synthesis and characterization of zinc oxide nanoparticles: Application to textiles as UV-absorbers. *Journal of Nanoparticle Research*, *10*(4), 679–689.
Belcher, R., Macdonald, A. M. G., Phang, S. E., & West, T. S. (1965). Submicro-methods for the analysis of organic compounds. Part xx. The determination of phosphorus and arsenic. *Journal of the Chemical Society*, *3*(6), 2044–2048.
Chen, D.-Q., Wang, Y.-Z., Hu, X.-P., Wang, D.-Y., Qu, M.-H., & Yang, B. (2005). Flame-retardant and anti-dripping effects of a novel char-forming flame retardant for the treatment of poly(ethylene terephthalate) fabrics. *Polymer Degradation and Stability*, *88*(2), 349–356.
Chruściel, J. J., & Leśniak, E. (2012). Modification of thermoplastics with reactive silanes and siloxanes. In P. A. El-Sonbati (Ed.), *Thermoplastic elastomers*. Rijeka, Croatia: InTech: Europe University Campus STeP Ri, Slavka Krautzeka 83/A.
Cook, J. G. (1984). *Natural fibres of vegetable origin*. *Handbook of textile fibres* (vol. I) Merrow, Shildon, England: Natural Fibres.
El-Sheikh, M. A. (2010). Carboxymethylation of maize starch at mild conditions. *Carbohydrate Polymers*, *79*(4), 875–881.
Gaan, S., & Sun, G. (2007a). Effect of phosphorus and nitrogen on flame retardant cellulose: A study of phosphorus compounds. *Journal of Analytical and Applied Pyrolysis*, *78*(2), 371–377.
Gaan, S., & Sun, G. (2007b). Effect of phosphorus flame retardants on thermo-oxidative decomposition of cotton. *Polymer Degradation and Stability*, *92*(6), 968–974.
Hsiue, G.-H., Liu, Y.-L., & Tsiao, J. (2000). Phosphorus-containing epoxy resins for flame retardancy V: Synergistic effect of phosphorus–silicon on flame retardancy. *Journal of Applied Polymer Science*, *78*(1), 1–7.
Hsiue, G. H., Liu, Y. L., & Liao, H. H. (2001). Flame-retardant epoxy resins: An approach from organic–inorganic hybrid nanocomposites. *Journal of Polymer Science Part A: Polymer Chemistry*, *39*(7), 986–996.
Jagst, E. (2011). *Surface functional group characterization using chemical derivatization X-ray photoelectron spectroscopy (cd-xps)*. Berlin: BAM Bundesanstalt für Materialforschung und -prüfung (Vol. MSc).
Jung, H.-S., Moon, D.-S., & Lee, J.-K. (2012). Quantitative analysis and efficient surface modification of silica nanoparticles. *Journal of Nanomaterials*, *2012*, 8.
Kathiervelu, S. S. (2003). Applications of nanotechnology in fibre finishing. *Synthetic Fibres*, *32*(4), 20–22.
Kathirvelu, S., D'Souza, L., & Dhurai, B. (2009). UV protection finishing of textiles using Zno nanoparticles. *Indian Journal of Fibre & Textile Research*, *34*(3), 274–278.
Knittel, D., & Schollmeyer, E. (2000). Technologies for a new century. Surface modification of fibres. *The Journal of the Textile Institute*, *91*(3), 151–165.
Liu, Y.-L., Hsiue, G.-H., Lee, R.-H., & Chiu, Y.-S. (1997). Phosphorus-containing epoxy for flame retardant. III: Using phosphorylated diamines as curing agents. *Journal of Applied Polymer Science*, *63*(7), 895–901.
Mahltig, B., & Böttcher, H. (2002). Refining of textiles by nanosol coating. *Melliand Textilberichte*, *83*(4), E50–E51.
Mohamed, A. L., Er-Rafik, M., & Moller, M. (2013a). Suitability of confocal Raman microscopy for monitoring the penetration of PDMS compounds into cotton fibres. *Carbohydrate Polymers*, *96*(1), 305–313.
Mohamed, A. L., Er-Rafik, M., & Moller, M. (2013b). Supercritical carbon dioxide assisted silicon based finishing of cellulosic fabric: A novel approach. *Carbohydrate Polymers*, *98*, 1095–1107.
Navarro, R. R., Tatsumi, K., Sumi, K., & Matsumura, M. (2001). Role of anions on heavy metal sorption of a cellulose modified with poly(glycidyl methacrylate) and polyethyleneimine. *Water Research*, *35*(11), 2724–2730.
Nelson, G. (2001). Microencapsulation in textile finishing. *Rev. Prog. Color.*, *31*, 57–64.
O'Connell, D. W., Birkinshaw, C., & O'Dwyer, T. F. (2006). A chelating cellulose adsorbent for the removal of cu(II) from aqueous solutions. *Journal of Applied Polymer Science*, *99*(6), 2888–2897.
Powell, C. S. (1998). Phosphorus-based flame retardants for textiles. *American Dyestuf Reporter*, *87*(9), 51–53.
Punyacharoennon, P., Charuchinda, S., & Srikulkit, K. (2010). Phosphonic acid functionalization of hyperbranched polyamidoamine grafted ultrafine silica to prepare the flame retardant for cotton fabric. In *The 2nd RMUTP International Conference: Green Trends in Foods, Crafts, Fashion & Textiles, vol. 2* Hotel Novotel Bangkok, Thailand.
Shukla, S. R., & Athalye, A. R. (1994). Graft-copolymerization of glycidyl methacrylate onto cotton cellulose. *Journal of Applied Polymer Science*, *54*(3), 279–288.
Sidney, S. (1967). *Quantitative organic analysis*. New York, USA: Wiley Interscience.
Simon, A., Cohen-Bouhacina, T., Porté, M. C., Aimé, J. P., & Baquey, C. (2002). Study of two grafting methods for obtaining a 3-aminopropyltriethoxysilane monolayer on silica surface. *Journal of Colloid and Interface Science*, *251*(2), 278–283.
Singh, V., Tiwari, A., Tripathi, D. N., & Sanghi, R. (2004). Microwave assisted synthesis of guar-g-polyacrylamide. *Carbohydrate Polymers*, *58*(1), 1–6.
Stober, W., Fink, A., & Bohn, E. (1968). Controlled growth of monodisperse silica spheres in the micron size range. *Journal of Colloid and Interface Science*, *26*, 62–69.
Stowell, J. K., & Yang, C. Q. (2003). A durable low-formaldehyde flame retardant finish for cotton fabrics. *AATCC Review*, *3*(2), 17–20.
Vogel, A. I. (1957). *Elementary practical organic chemistry, part (3), quantitive organic analysis*. London: Longman Group Ltd.
Wang, X.-L., Huang, Y., Zhu, J., Pan, Y.-B., He, R., & Wang, Y.-Z. (2009). Chitosan-graft poly(p-dioxanone) copolymers: Preparation, characterization, and properties. *Carbohydr Res*, *344*(6), 801–807.
Wu, C. S., Liu, Y. L., & Chiu, Y. S. (2002). Epoxy resins possessing flame retardant elements from silicon incorporated epoxy compounds cured with phosphorus or nitrogen containing curing agents. *Polymer*, *43*(15), 4277–4284.
Yang, G., & Zhai, H. M. (2012). Synthesis and properties of glycidyl methacrylate grafted eucalyptus fiber. *Cellulose Chemistry and Technology*, *46*(3–4), 243–248.
Zhu, P., Sui, S., Wang, B., Sun, K., & Sun, G. (2004). A study of pyrolysis and pyrolysis products of flame-retardant cotton fabrics by DSC, TGA, and py-gc-ms. *Journal of Analytical and Applied Pyrolysis*, *71*(2), 645–655.